Distribution of Cell Size in Bounded Poisson Voronoi Tessellations with Application to Secure Local Connectivity

Konstantinos Koufos and Carl P. Dettmann

Abstract

We consider the Voronoi tessellation induced by a homogeneous and stationary Poisson point process of intensity $\lambda > 0$ in a quadrant, where the two half-axes represent boundaries. We show that the mean cell size is less than λ^{-1} when the seed is located exactly at the boundary, and it can be larger than λ^{-1} when the seed lies close to the boundary. In addition, we calculate the second moment of the cell size at two locations: (i) at the corner of a quadrant, and (ii) at the boundary of the half-plane. In both cases, we illustrate that the two-parameter Gamma distribution, with location-dependent parameters, provides a good fit. As a potential application, we use the Gamma approximations to study the degree distribution for secure in-connectivity in wireless sensor networks deployed over a bounded domain.

Index Terms

Physical layer security, Poisson Voronoi tessellations, stochastic geometry

I. INTRODUCTION

A random tessellation is a random subdivision of a space into disjoint regions or cells $\mathcal{C}_i$, see [1], [2] for a formal definition. Perhaps the most basic random tessellation model partitions the plane $\mathbb{R}^2$ into Voronoi cells. In order to construct them, a set of random nuclei (or seeds) S_i are first distributed, and then, the locations of the plane are associated with the nearest seed for the Euclidean distance. The boundaries of the Voronoi cells are equidistant to the two nearest

K. Koufos and C.P. Dettmann are with the School of Mathematics, University of Bristol, BS8 1TW, Bristol, UK. {K.Koufos, Carl.Dettmann}@bristol.ac.uk

seeds. When the distribution of the seeds follows the stationary Poisson Point Process (PPP) with a finite intensity $\lambda > 0$, the random tessellation is widely-known as the Poisson Voronoi Tessellation (PVT) [1], [2]. Since the concept of PVT is quite fundamental, it accepts a wide range of applications from geo-sciences and astronomy, e.g., [3], [4] to telecommunications [5].

The statistical properties of planar PVTs, e.g., cell area, perimeter, vertex degree, etc. have been studied since the early 1950's [6], [7]. The Probability Distribution Function (PDF) of the area of the typical cell in a planar PVT is unknown, and approximations using the Gamma and the log-normal distribution with appropriately selected parameters have been widely adopted [8]–[11]. An intuitive explanation for the good fit of the Gamma distribution using the nearest neighbour approximation is presented in [8]. In [12], an integral-based method is devised to compute various statistics of the PVT including the edge length, the PDFs of the distance and angle between neighbouring seeds and vertices, the cell size etc. Unlike the PVT, the distribution of cell size in planar Poisson Delaunay tessellation is known; it can be expressed in terms of the modified Bessel function [13]. For three-dimensional Delaunay cells, some properties of geometrical characteristics are available in [14].

Following the recent emergence of small cell wireless networks with irregular structure, fundamental tools from stochastic geometry have been adopted to model the deployment of network elements and assess the performance [15]. The Gamma approximation for the distribution of cell size in PVTs has been used in cellular systems, e.g., to approximate the PDF of the network load in a typical Voronoi cell [16], as well as in Wireless Sensor Networks (WSN), e.g., to investigate the PDF of in-degree for secure local connectivity [17]. Nevertheless, small cell wireless networks have boundaries, and the statistics of a typical Voronoi cell may not well represent the properties of cells located close to the network borders.

In this paper, we consider a PVT over a quadrant, where the two half-axes represent boundaries. We assume that the location of a seed of the underlying PPP, hereafter the seed S_0, is arbitrarily fixed either at the boundary or close to the boundary. Firstly, we extend the integral-based method in [12] to compute the mean cell size. Unlike the PVTs in the infinite plane, we show that a unit-intensity PPP in a quadrant can induce Voronoi cells with mean area smaller or larger than unity. Secondly, we show how to compute the second moment of the cell size for the Voronoi cell $\mathcal{C}_0$ (that generated by seed S_0) assuming that the seed S_0 is located either at the corner of the quadrant or at the boundary and far from the corner. The latter can be seen as a PVT in the half-plane with the seed S_0 located at the boundary. In both cases, we illustrate that the Gamma

distribution with fitted mean and variance provides an accurate approximation for the distribution of the cell size. In a recent paper [18], it has been shown that the asymptotic distribution of the Voronoi cell size is independent of the location of the seed S_0 (almost everywhere) and of the intensity underlying the PPP including also the case of inhomogeneous PPP. Our results complement the analysis in [18], showing that for a homogeneous PPP with finite intensity λ and in a zero measure set of S_0, i.e., at the boundary, the moments of the cell size can be location-dependent.

As a potential application, we utilize the Gamma approximation to study the distribution of in-degree with physical layer security in WSN [19]. We illustrate that for a sensor located at the boundary, it might be more probable to have secure out-connectivity than secure in-connectivity. This result complements the analysis in [17], where it is shown that in the infinite plane, secure in-connectivity is more probable than out-connectivity.

II. POISSON VORONOI TESSELLATION OVER A QUADRANT

We consider a PVT of unit intensity (without loss of generality) over the quadrant $\mathbb{R}_+^2$. We denote by $\mathcal{S}$ the set of seeds S_i generating the Voronoi cells, i.e., $S_i \in \mathcal{S}, i = 0, 1, \ldots,$. Due to the Slivnyak's Theorem, see for instance [20], the statistical properties of the PPP do not change by conditioning the location of a seed. In order to study the properties of Voronoi cells close to the boundary, let us assume that the seed S_0 (that generating the Voronoi cell $\mathcal{C}_0$) is located (i) along the boundary at distance $a \geq 0$ from the corner of the quadrant, (ii) at distance $h \geq 0$ from the boundary of the half-plane. The latter can also be seen as the case where the seed S_0 is located far from the corner of the quadrant and at distance h from the boundary. Let us consider a point $P \in \mathbb{R}_+^2$ with polar coordinates (r, ϕ). The point P can be interior to some cell, at the boundary separating two cells, or it can also be a vertex. Adopting the terminology used in [12], we define the *void* of the point P to be the intersection of the quadrant $\mathbb{R}_+^2$, and the disk with center that point and radius equal to the distance to the nearest seed(s). We denote by A the area of the cell $\mathcal{C}_0$. In the next section, we show how to calculate the mean area $\mathbb{E}\{A\}$.

III. MEAN CELL SIZE

In order to compute the mean area of the cell $\mathcal{C}_0$, we should identify the probability that the point P is interior to the cell $\mathcal{C}_0$ and integrate this probability over the quadrant. The point P is interior to that cell when its void is empty of other seeds, and the seed S_0 lies on its
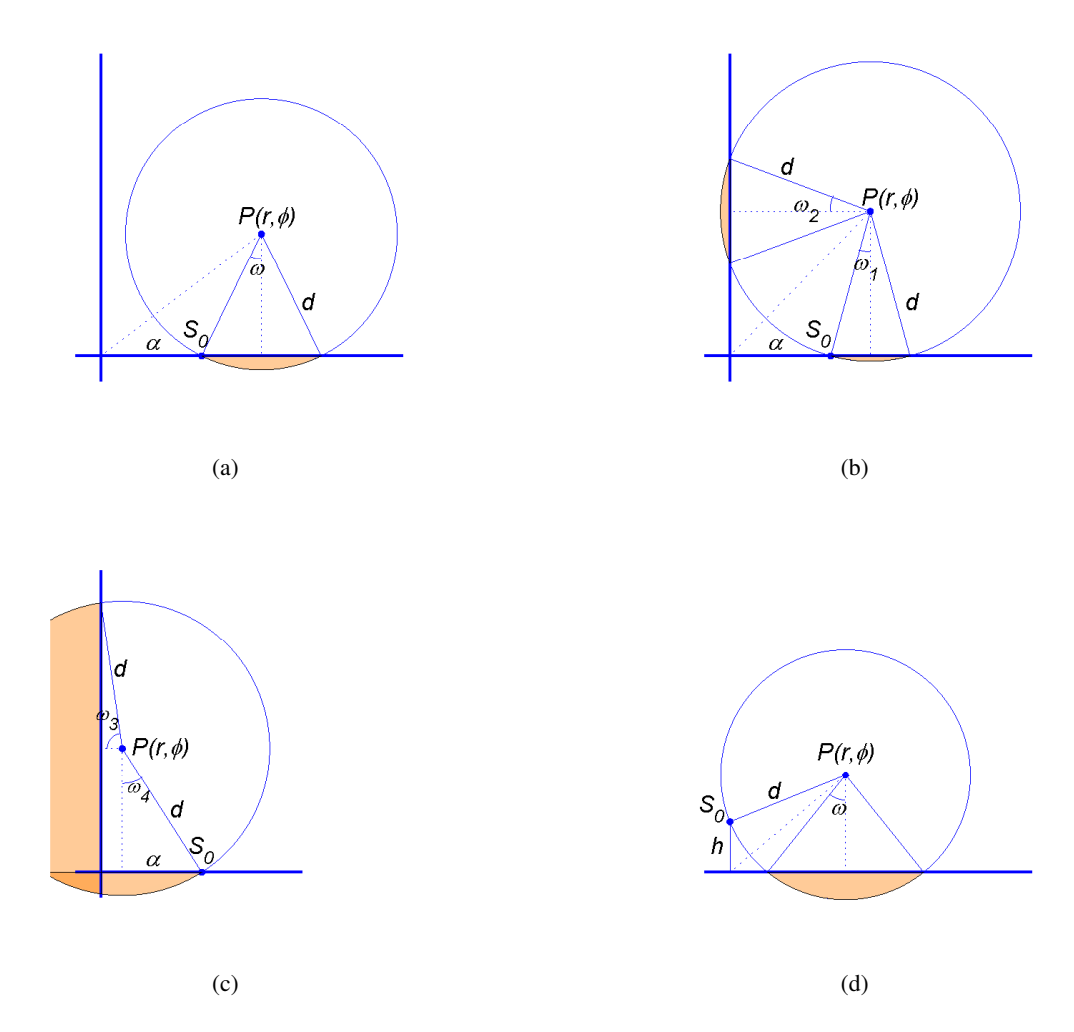
Fig. 1. Coordinate systems and example illustrations of the void area around an interior point P. In (a)−(c) the seed S_0 is located at distance a from the corner of the quadrant. In (d), the seed S_0 is located at distance h from the boundary of the half-plane.

circumference. Since the underlying PPP has unit intensity, the probability that the void of the point P is empty is $e^{-V(P)}$, where the size of the void is $V(P) = D\left(P, d\left(P, S_0\right)\right) \cap \mathbb{R}_+^2$. The mean cell size can be read as

$$\mathbb{E}\{A\} = \mathbb{E}\left[\int_{\mathbb{R}_+^2} \mathbb{1}_{P \in \mathcal{C}_0} \mathrm{d}P\right] = \int_{\mathbb{R}_+^2} \mathbb{P}\left(P \in \mathcal{C}_0\right) \mathrm{d}P = \int_{\mathbb{R}_+^2} e^{-V(P)} \mathrm{d}P.$$

Let us assume that the seed S_0 is located along the boundary at distance a from the corner. Given the distance a, we separate between the following cases in the calculation of the size of the area $V(P)$:

- $r \geq a/2, \phi \leq \phi_1$, where $\phi_1 = \arccos\left(\frac{-a+\sqrt{2a^2+r^2}}{r}\right)$ is obtained as the positive solution of the equation $d = r\cos\phi$, where $d = \sqrt{r^2 + a^2 - 2ar\cos\phi}$ is the distance between S_0 and P. For $\phi = \phi_1$ the void becomes tangential to the boundary along the y-axis. For $\phi \leq \phi_1$, the boundary along the x-axis cuts some part of the void, see Fig. 1(a). The angle ω in Fig. 1(a) can be calculated as $\omega = \arccos\left(\frac{r\sin\phi}{d}\right)$, and the size of the void, denoted by V_1, is

$$V_1 = \pi d^2 - \omega d^2 + r\sin\phi \left| r\cos\phi - a \right|. \tag{1}$$

- $r \geq a/2, \phi_1 \leq \phi \leq \phi_2$, where the angle $\phi_2 = \arccos\left(\frac{a}{2r}\right)$ is the solution of $d = \sqrt{r^2 + a^2 - 2ar\cos\phi}$ for $d = r$. For $\phi = \phi_2$, the circle $D(P, d(P, S_0))$ passes through the corner of the quadrant. For $\phi_1 \leq \phi \leq \phi_2$, both boundaries along the x- and y-axis determine the void, see Fig. 1(b). In Fig. 1(b), $\omega_1 = \omega$, $\omega_2 = \arccos\left(\frac{r\cos\phi}{d}\right)$, and the size of the void, denoted by V_2, is

$$V_2 = \pi d^2 - (\omega_1 + \omega_2) d^2 + r\sin\phi \left| r\cos\phi - a \right| + rd\cos\phi\sin\omega_2. \tag{2}$$

- $r \geq a/2, \phi_2 \leq \phi \leq \pi/2$. In that case, see Fig. 1(c), the size of the void, denoted by V_3, can be calculated as the sum of a trapezium, a triangle and a circular domain with radius d and angle $\left(\frac{3\pi}{2} - \omega_3 - \omega_4\right)$, where $\omega_3 = \omega_2$ and $\omega_4 = \omega$. Hence,

$$V_3 = \frac{1}{2}r\sin\phi\left(r\cos\phi + a\right) + \frac{1}{2}rd\cos\phi\sin\omega_3 + \frac{\frac{3\pi}{2} - \omega_3 - \omega_4}{2\pi}\pi d^2. \tag{3}$$

- $r \leq a/2, \phi \leq \pi/2$. In that case, $\phi_1 = \phi_2 = 0$, and the void of the point P always contains the corner of the quadrant in its interior. The size of the void is still given by equation (3).

Finally, one has to sum up the four terms to consider all points in the quadrant.

$$\mathbb{E}\{A\} = \int_0^{\phi_1}\int_{\frac{a}{2}}^\infty e^{-V_1}r\mathrm{d}r\mathrm{d}\phi + \int_{\phi_1}^{\phi_2}\int_{\frac{a}{2}}^\infty e^{-V_2}r\mathrm{d}r\mathrm{d}\phi + \int_{\phi_2}^{\frac{\pi}{2}}\int_{\frac{a}{2}}^\infty e^{-V_3}r\mathrm{d}r\mathrm{d}\phi + \int_0^{\frac{\pi}{2}}\int_0^{\frac{a}{2}} e^{-V_3}r\mathrm{d}r\mathrm{d}\phi. \tag{4}$$

Lemma 1. *For a PVT induced by a unit-intensity PPP in the quadrant $\mathbb{R}_+^2$, the mean size of the cell $\mathcal{C}_0$ is $\frac{\arccos\left(\frac{2}{\pi}\right)}{\sqrt{\pi^2-4}}$ when the seed S_0 is located at the corner.*

Proof. When the seed S_0 is located at the corner of the quadrant, one may substitute $a = 0$, $\phi_1 = 0$ and $\phi_2 = \pi/2$ in equation (4). Therefore the size of the void area is essentially computed from equation (2) after substituting $d = r$, $\omega_1 = \frac{\pi}{2} - \phi$ and $\omega_2 = \phi$. The mean cell size is finally expressed as

$$\mathbb{E}\{A\} = \int_0^{\pi/2}\int_0^\infty e^{-r^2\left(\frac{\pi}{2}+\sin(2\phi)\right)}r\mathrm{d}r\mathrm{d}\phi = \frac{\arccos\left(\frac{2}{\pi}\right)}{\sqrt{\pi^2-4}} \approx 0.36351. \tag{5}$$
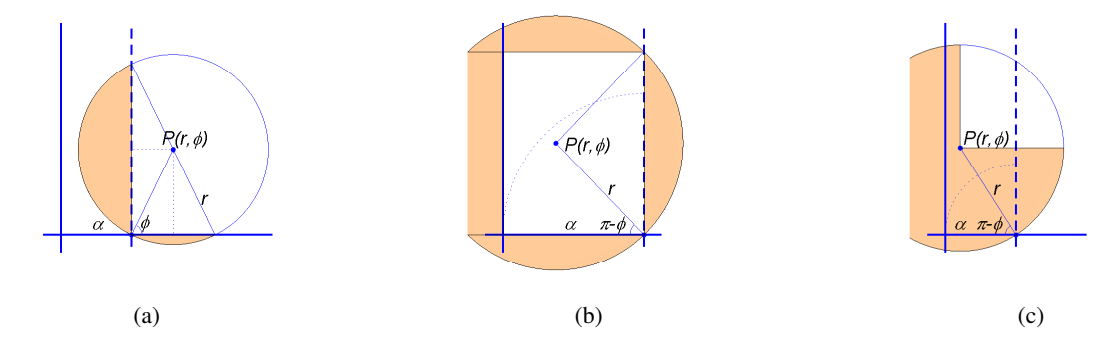
Fig. 2. Example illustrations in the calculation of the upper bound for the mean cell size in Lemma 2.

□

Lemma 2. *For a PVT induced by a unit-intensity PPP in the quadrant $\mathbb{R}_+^2$, the mean size of the cell $\mathcal{C}_0$ is less than unity when the seed S_0 is located at the boundary.*

Proof. In order to compute an upper bound for the mean cell size in equation (4) for arbitrary $a \geq 0$, we change the coordinate system so that the seed S_0 becomes the origin, and we construct lower bounds for the size of the void areas which can be evaluated in closed- and/or semi-closed form. We will consider all points of the quadrant. Note that the coordinates of the boundaries of the quadrant is $x = -a$ and $y = 0$ in the new coordinate system, see Fig. 2.

When $r \geq 0, 0 \leq \phi \leq \frac{\pi}{2}$ in the new coordinate system, see Fig. 2(a), we construct a lower bound for the size of the void area considering that the y-axis, $x = 0$, see the dashed line in Fig. 2(a), is a boundary. Thus, the mean cell size due to these points of the quadrant is actually bounded by equation (5).

In order to bound the size of the void for $0 \leq r \leq a, \frac{\pi}{2} \leq \phi \leq \pi$, see Fig. 2(b), we use the area of the rectangle with sides a and $2r\sin\phi$. Thus, the contribution of these points to the bound is equal to

$$\int_0^a \int_{\frac{\pi}{2}}^{\pi} e^{-2ar\sin\phi} r \mathrm{d}r \mathrm{d}\phi = -\frac{\pi}{4} \mathbf{M}_1\left(2a^2\right),$$

where $\mathbf{M}_\nu(x)$ is the modified Struve function of the second kind, $\mathbf{M}_\nu(x) = \mathbf{L}_\nu(x) - I_\nu(x)$, where $\mathbf{L}_\nu(x)$ is the modified Struve function of the first kind, see [24, pp. 498], and $I_\nu(x)$ is the modified Bessel function of the first kind, see [24, pp. 374].

For the remaining points of the quadrant, i.e, $r > a$, $\frac{\pi}{2} \leq \phi \leq \pi - \arccos\left(\frac{a}{r}\right)$, see Fig. 2(c), a lower bound on the size of the void area is obtained by considering just a quarter of the circle. Hence, the remaining points give a contribution equal to

$$\int_a^\infty \int_{\frac{\pi}{2}}^{\pi - \arccos\left(\frac{a}{r}\right)} e^{-\frac{\pi}{4}r^2} r \mathrm{d}\phi \mathrm{d}r = e^{-\frac{a^2\pi}{4}} - \mathrm{Erfc}\left(\frac{a\sqrt{\pi}}{2}\right),$$

where $\mathrm{Erfc}(x) = \frac{2}{\sqrt{\pi}} \int_x^\infty e^{-t^2} \mathrm{d}t$ is the complementary error function.

After summing up the contributions from the three parts of the quadrant we get

$$\mathbb{E}\{A\} < e^{-\frac{a^2\pi}{4}} - \mathrm{Erfc}\left(\frac{a\sqrt{\pi}}{2}\right) - \frac{\pi}{4}\mathbf{M}_1\left(2a^2\right) + \frac{\arccos\left(\frac{2}{\pi}\right)}{\sqrt{\pi^2 - 4}}. \tag{6}$$

The upper bound in (6) can be evaluated at arbitrary precision, and it is less than unity for all $a \geq 0$, see the red line in Fig. 3(a). As $a \to \infty$, the Struve function converges to $\lim_{a\to\infty} \mathbf{M}_1(2a^2) = -\frac{2}{\pi}$, and the bound converges to $\frac{1}{2} + \frac{\arccos\left(\frac{2}{\pi}\right)}{\sqrt{\pi^2-4}}$. □

Lemma 3. *For a PVT induced by a unit-intensity PPP in the half-plane, the mean size of cell $\mathcal{C}_0$ is less than unity when the seed S_0 is located at the boundary.*

Proof. To simplify integration, we take a coordinate system where the seed S_0 is the origin. The size of the void area for points with coordinates $r \geq 0$, $0 \leq \phi \leq \pi/2$ can be calculated using equation (1) after substituting $d = r$, $a = 0$ and $\omega = \frac{\pi}{2} - \phi$. After some straightforward calculation we get

$$\mathbb{E}\{A\} = 2 \int_0^{\pi/2} \int_0^\infty e^{-r^2\left(\frac{\pi}{2} + \phi + \sin(\phi)\cos(\phi)\right)} r \mathrm{d}r \mathrm{d}\phi = \int_0^{\pi/2} \frac{2\mathrm{d}\phi}{\pi + 2\phi + \sin(2\phi)} \approx 0.61082, \tag{7}$$

where we have multiplied by 2 to account for the angles $\pi/2 \leq \phi \leq \pi$.

One may also note that $\mathbb{E}\{A\} < \int_0^{\frac{\pi}{2}} \frac{2\mathrm{d}\phi}{\pi + 2\phi} = \log(2) < 1$. Another way to prove that $\mathbb{E}\{A\} < 1$ is to take the limit of the bound in (6) as $a \to \infty$, resulting to $\mathbb{E}\{A\} < \frac{1}{2} + \frac{\arccos\left(\frac{2}{\pi}\right)}{\sqrt{\pi^2-4}} < 1$. □

Remark 1. *A rather loose lower bound to equation* (4) *can be obtained after neglecting the impact of the boundaries on the size of the void and substituting $V_1 = V_2 = V_3 = \pi d^2$ in equation* (4). *Finally, $\mathbb{E}\{A\} > \frac{1}{4}\left(1 + Erf(a\sqrt{\pi})\right) \forall a \geq 0$, where $Erf(x) = \frac{2}{\sqrt{\pi}} \int_0^x e^{-t^2} \mathrm{d}t$ is the error function.*

The computation of the mean cell size for varying a using equation (4) is validated in Fig. 3(a). One may also find there the lower bound, see Remark 1, and the upper bound, see (6), to the mean cell size. We see that for large a, the mean converges to the value given in equation (7).
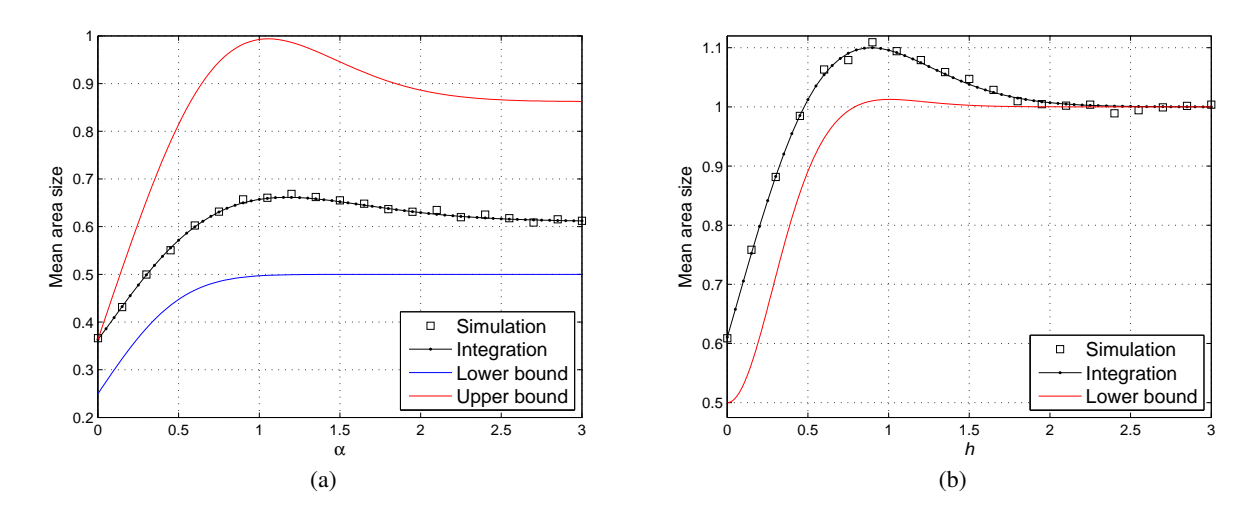
Fig. 3. The integral-based calculation in equations (4) and (8) is verified by simulations. Mean cell size w.r.t. (a) the distance a from the corner of the quadrant, (b) the distance h from the boundary of the half-plane. The PPP intensity is unity, $\lambda = 1$. In the simulations, we consider a square with side $L = 10$. The PVT and the area of the cell $\mathcal{C}_0$ are simulated using MatLab toolboxes. Given the set of seeds, the algorithm identifies the vertices and the boundary intersection points, and calculates the area of the polygon associated with the cell $\mathcal{C}_0$. In the simulations for varying h, the coordinates of the seed $\mathcal{S}_0$ are taken equal to $\left(\frac{L}{2}, h\right)$.

For small a, e.g., $a \leq \frac{1}{2}$, the vertical boundary reduces significantly the mean cell size. For intermediate values of a, e.g., $1 \leq a \leq 2$, the mean cell size is large when the cell $\mathcal{C}_0$ contains also the corner of the quadrant in its interior.

Let us now assume that the seed S_0 is located at distance h from the boundary of the half-plane, see Fig. 1(d). In order to simplify the integration, we assume that the origin of the coordinate system is the point at the boundary nearest to S_0, thus the polar coordinates of S_0 become $\left(h, \frac{\pi}{2}\right)$. By following similar steps used to obtain equations (1)−(4), one can show that the mean cell size as a function of the parameter h is

$$\mathbb{E}\{A\} = 2\int_0^{\phi_0}\int_{h/2}^{\infty} e^{-V_1} r \mathrm{d}r \mathrm{d}\phi + 2\int_{\phi_0}^{\pi/2}\int_{h/2}^{\infty} e^{-V_2} r \mathrm{d}r \mathrm{d}\phi + 2\int_0^{\pi/2}\int_0^{h/2} e^{-V_1} r \mathrm{d}r \mathrm{d}\phi, \tag{8}$$

where $V_1 = \left(\pi - \omega + \frac{\sin(2\omega)}{2}\right)d^2$, $V_2 = \pi d^2$, $d = \sqrt{r^2 + h^2 - 2hr\sin\phi}$, $\phi_0 = \arcsin\left(\frac{-h + \sqrt{2h^2 + r^2}}{r}\right)$, $\omega = \arccos\left(\frac{r\sin\phi}{d}\right)$, and the factor 2 has been added to account for angles $\pi/2 \leq \phi \leq \pi$.

Lemma 4. *For a PVT induced by a unit-intensity PPP in the half plane, the mean size of the cell $\mathcal{C}_0$ can be larger than unity when the seed S_0 lies close to the boundary.*

Proof. First, we note that the lower bound obtained by setting $V_1 = V_2 = \pi d^2$ in equation (8)
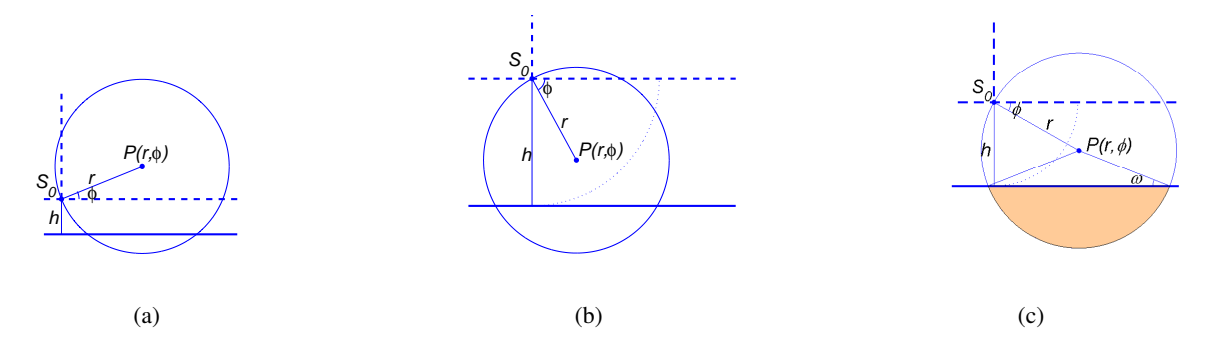
Fig. 4. Example illustrations in the calculation of the lower bound for the mean cell size in Lemma 4.

is equal to $\frac{1}{2}\left(1 + \mathrm{Erf}\left(h\sqrt{\pi}\right)\right) \forall h \geq 0$. This is increasing in h becoming unity as $h \to \infty$, thus cannot be used to claim mean cell sizes larger than unity. In order to obtain a lower bound to equation (8) which is larger than unity for some h, we change the coordinate system so that the seed S_0 becomes the origin, and we construct appropriate upper bounds for the size of the void areas. In the new system, see the dashed lines in Fig. 4(a)$-$4(c), the coordinates of the boundary is $y = -h$.

When $r \geq 0, 0 \leq \phi \leq \frac{\pi}{2}$, see Fig. 4(a), we may neglect the impact of boundary on the size of the void with negligible approximation error, thus

$$2 \int_0^\infty \int_0^{\frac{\pi}{2}} e^{-\pi r^2} r \mathrm{d}r \mathrm{d}\phi = \frac{1}{2}.$$

When $r \leq h, -\frac{\pi}{2} \leq \phi \leq 0$, see Fig. 4(b), we still neglect the impact of boundary on the size of the void. Note that this approximation may introduce non-negligble error for the points with radii $\frac{h}{2} \leq r \leq h$.

$$2 \int_0^h \int_{-\frac{\pi}{2}}^0 e^{-\pi r^2} r \mathrm{d}r \mathrm{d}\phi = \frac{1}{2}\left(1 - e^{-\pi h^2}\right).$$

Finally, for the remaining points $r \geq h, -\arcsin\left(\frac{h}{r}\right) \leq \phi \leq 0$, see Fig. 4(c), the size of the void area is $V(\phi) = \left(\frac{\pi}{2} + \omega + \cos\omega\sin\omega\right) r^2$, where $\omega(\phi) = \arcsin\left(\frac{h}{r} + \sin\phi\right)$. Due to the fact that $\frac{1}{2}\sin(2x) < x \,\forall x \geq 0$, the size of the void area can be upper-bounded by $V(\phi) \leq \left(\frac{\pi}{2} + 2\omega\right) r^2$. For $r \geq h, -\frac{\pi}{2} \leq -\arcsin\left(\frac{h}{r}\right) \leq \phi \leq 0$, the function $\omega(\phi)$ is increasing in ϕ with positive second derivative. Hence, $V(\phi) \leq \left(\frac{\pi}{2} + 2\left(\arcsin\left(\frac{h}{r}\right) + \phi\right)\right) r^2$. Therefore the contribution of the remaining points to the mean cell size can be lower-bounded as

$$\int_h^\infty \int_{-\arcsin\left(\frac{h}{r}\right)}^0 e^{-\left(\frac{\pi}{2} + 2\left(\arcsin\left(\frac{h}{r}\right) + \phi\right)\right) r^2} r \mathrm{d}\phi \mathrm{d}r = \frac{1}{2}\mathrm{Ei}\left(\frac{\pi h^2}{2}\right) - \int_h^\infty \frac{1}{r} e^{-\left(\frac{3\pi}{2} - 2\arccos\left(\frac{h}{r}\right)\right) r^2} \mathrm{d}r,$$

where $\mathrm{Ei}(x) = \int_x^\infty \frac{e^{-t}}{t} \mathrm{d}t, x > 0$ is the exponential integral.

In order to lower bound the right-hand side of the equation above, we need to upper bound the second term. A rather trivial upper bound is obtained using a piecewise function to upper-bound $\arccos\left(\frac{h}{r}\right)$, i.e, $\frac{\pi}{3}$ for $h \leq r \leq 2h$ and $\frac{\pi}{2}$ for $r > 2h$.

$$\int_h^\infty \frac{1}{r} e^{-\left(\frac{3\pi}{2} - 2\arccos\left(\frac{h}{r}\right)\right)r^2} \mathrm{d}r < \frac{1}{2}\left(\mathrm{Ei}\left(\frac{5\pi h^2}{6}\right) - \mathrm{Ei}\left(\frac{10\pi h^2}{3}\right) + \mathrm{Ei}\left(2\pi h^2\right)\right)$$

After summing up the contributions from the three parts of the half-plane we get

$$\begin{aligned} \mathbb{E}\{A\} \quad > \quad & 1 - \tfrac{1}{2}e^{-\pi h^2} + \tfrac{1}{2}\left(\mathrm{Ei}\left(\tfrac{10\pi h^2}{3}\right) - \mathrm{Ei}\left(\tfrac{5\pi h^2}{6}\right) + \right. \\ & \left. \mathrm{Ei}\left(\tfrac{\pi h^2}{2}\right) - \mathrm{Ei}(2\pi h^2)\right). \end{aligned} \tag{9}$$

The right-hand side of (9) can be evaluated at arbitrary precision. When the distance h to the boundary is around $h = 1$, we observe mean cell sizes larger than unity, see Fig. 3(b). □

Remark 2. *In Fig. 3, we see that the integral-based calculation matches quite well the simulation results even for a moderate average number of points, $\lambda L^2 = 100$, inside the square. Note that the probability of a void region touching opposite sides of the square is at most $\exp(-\lambda \pi L^2/2)$, thus negligible for our parameter settings.*

IV. SECOND MOMENT OF CELL SIZE

In order to calculate the second moment of the cell size, one has to consider two points $P_1(r_1, \phi_1)$, $P_2(r_2, \phi_2)$ interior to the cell $\mathcal{C}_0$.

$$\mathbb{E}\{A^2\} = \int_{\mathbb{R}_+^2 \times \mathbb{R}_+^2} \mathbb{P}(P_1, P_2 \in \mathcal{C}_0) \, \mathrm{d}P_1 \mathrm{d}P_2 = \int_{\mathbb{R}_+^2 \times \mathbb{R}_+^2} e^{-V(P_1, P_2)} \mathrm{d}P_1 \mathrm{d}P_2,$$

where $V(P_1, P_2) = [D(P_1, d(P_1, S_0)) \cup D(P_2, d(P_2, S_0))] \cap \mathbb{R}_+^2$ is the size of the intersection area of the two disks and the quadrant, and the points S_0, P_1, P_2 cannot be collinear.

In the infinite plane, the calculation of the second moment using integral-based methods can be found in [12], [21]. The computation of the void area $V(P_1, P_2)$ in a bounded domain is cumbersome. Nevertheless, when the seed S_0 is fixed either at the corner of the quadrant, $a = 0$, or at the boundary of the half-plane, $h = 0$, the second moment can still be calculated using few integration terms.

Lemma 5. *For a PVT induced by a unit-intensity PPP in the quadrant $\mathbb{R}_+^2$, the second moment of the size of the cell $\mathcal{C}_0$ when the seed S_0 is located at the corner is*

$$\mathbb{E}\{A^2\} = \int_0^{\frac{\pi}{2}} \int_{\theta - \frac{\pi}{2}}^{\theta} \int_{-\omega_1}^{\frac{\pi}{2} - \theta} \frac{f(\omega_1, \omega_2)\, \mathrm{d}\omega_2 \mathrm{d}\omega_1 \mathrm{d}\theta}{V_1^2} + 2 \int_{-\frac{\pi}{2}}^0 \int_{-\frac{\pi}{2}}^{\theta} \int_{-\omega_1}^{\frac{\pi}{2}} \frac{f(\omega_1, \omega_2)\, \mathrm{d}\omega_2 \mathrm{d}\omega_1 \mathrm{d}\theta}{V_2^2},$$
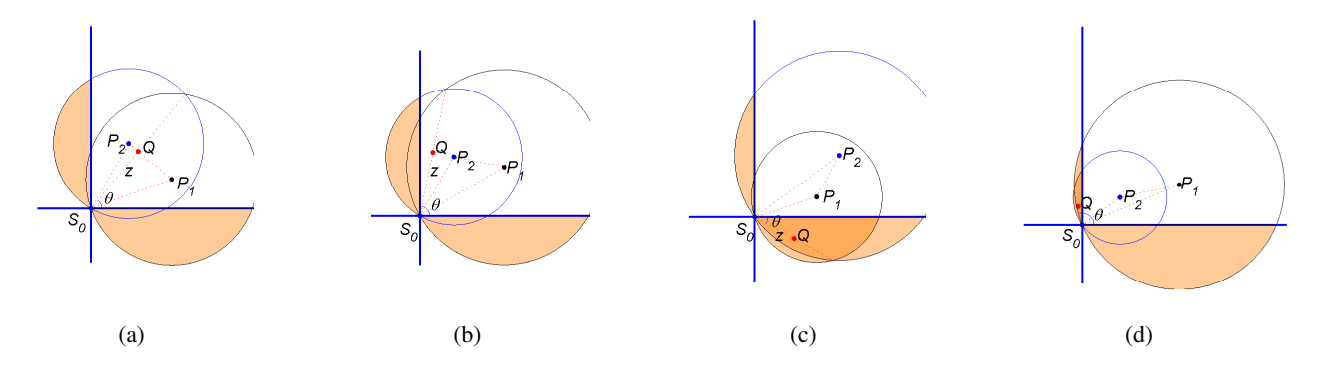
Fig. 5. Coordinate systems and example illustrations of the void area around two interior points P_1, P_2 when the seed S_0 is located at the origin of the quadrant.

where $V_1 = \frac{2\theta + \sin(2(\theta - \omega_1)) + \sin(2\omega_1)}{2\cos^2\omega_1} + \frac{\pi - 2\theta + \sin(2(\theta + \omega_2)) + \sin(2\omega_2)}{2\cos^2\omega_2}$, $V_2 = \frac{\pi + 2\sin(2(\theta + \omega_2))}{2\cos^2\omega_2}$, *and* $f(\omega_1, \omega_2) = \frac{\sin(\omega_1 + \omega_2)}{\cos^3\omega_1 \cos^3\omega_2}$.

Proof. We transform the coordinate system as follows: (z, θ) are the polar coordinates of the point Q which is the intersection point of the line passing through P_1, P_2 and its perpendicular line passing through the origin S_0, ω_1 is the angle QS_0P_1 measured clockwise, and ω_2 is the angle QS_0P_2 measured counter-clockwise, see Fig. 5 for example illustrations. The transformation can be read as $\phi_1 = \theta - \omega_1$, $\phi_2 = \theta + \omega_2$, $r_1 = \frac{z}{\cos\omega_1}$ and $r_2 = \frac{z}{\cos\omega_2}$. The determinant of the Jacobian matrix of the transformation is $|J| = z^3 f(\omega_1, \omega_2)$, where $f(\omega_1, \omega_2) = \frac{\sin(\omega_1 + \omega_2)}{\cos^3\omega_1 \cos^3\omega_2}$.

Due to the fact that $r_1 = \frac{z}{\cos\omega_1}$ and $r_2 = \frac{z}{\cos\omega_2}$, the size of the void can be written as $V_j z^2$, where V_j is the size normalized for $z = 1$. After integrating the probability of an empty void, $\int e^{-V_j z^2} z^3 f(\omega_1, \omega_2)\, \mathrm{d}P_1 \mathrm{d}P_2$, over $z \geq 0$, we get $\int \frac{f(\omega_1, \omega_2)}{2V_j^2} \mathrm{d}\omega_2 \mathrm{d}\omega_1 \mathrm{d}\theta$. In the infinite plane, or equivalently in the bulk of the deployment area, the size of the normalized void is

$$V = \frac{\pi + 2\omega_1 + \sin(2\omega_1)}{2\cos^2\omega_1} + \frac{\pi + 2\omega_2 + \sin(2\omega_2)}{2\cos^2\omega_2}.$$

Using the above equation, the second moment of the cell size in the infinite plane can be calculated approximately equal to 1.28 [12], [21]. When the seed S_0 is located at the corner of the quadrant, even though both points P_1, P_2 are located in the upper-right quadrant, the angle θ can take values in $\left[-\frac{\pi}{2}, \pi\right]$. The range of the variables ω_1, ω_2 depend on the quadrant where the point Q lies. Therefore the computation of the void can be divided into three parts. When the point Q lies in the upper-right quadrant, the angles ω_1, ω_2 could be positive or negative. Example illustrations are in Fig. 5(a), where the angle ω_2 is positive and in Fig. 5(b), where ω_2 is negative. In both figures, ω_1 is positive. In order to calculate the size of the void inside

the quadrant $\mathbb{R}_+^2$, we take the void generated by P_1 and subtract: (i) the shaded area under the x-axis, and (ii) the part of the void at the left of the line passing through S_0 and Q. In a similar manner, we can calculate the void contribution due to the point P_2. After summing up we get

$$V_1 = \frac{2\theta + \sin\left(2\left(\theta - \omega_1\right)\right) + \sin\left(2\omega_1\right)}{2\cos^2\omega_1} + \frac{\pi - 2\theta + \sin\left(2\left(\theta + \omega_2\right)\right) + \sin\left(2\omega_2\right)}{2\cos^2\omega_2}.$$

When the angle θ is negative, e.g., in Fig. 5(c), ω_1 becomes always negative and ω_2 always positive. In Fig. 5(c), we may see that the point P_1 can be ignored, and the size of the void can be calculated solely based on P_2, i.e., $V_2 = \frac{\pi + 2\sin(2(\theta + \omega_2))}{2\cos^2\omega_2}$. Finally, when $\frac{\pi}{2} \leq \theta \leq \pi$, see Fig. 5(d), the size of the void depends only on P_1, and $V_3 = \frac{\pi + 2\sin(2(\theta - \omega_1))}{2\cos^2\omega_1}$. Due to symmetry, negative angles, $\theta \leq 0$ and angles larger than $\frac{\pi}{2}$ give equal contributions. In addition, every integral term must be multiplied by two to consider each pair of points twice, and the Lemma is proved. $\qquad\square$

Lemma 6. *For a PVT induced by a unit-intensity PPP in the half-plane, the second moment of the size of the cell $\mathcal{C}_0$ when the seed S_0 is located at the boundary is*

$$\mathbb{E}\left\{A^2\right\} = \int_0^{\frac{\pi}{2}} \int_{\theta - \frac{\pi}{2}}^{\theta} \int_{-\omega_1}^{\frac{\pi}{2} - \theta} \frac{2f(\omega_1, \omega_2)\mathrm{d}\omega_2\mathrm{d}\omega_1\mathrm{d}\theta}{V_1^2} + \int_0^{\frac{\pi}{2}} \int_{\theta - \frac{\pi}{2}}^{\theta} \int_{\frac{\pi}{2} - \theta}^{\frac{\pi}{2}} \frac{2f(\omega_1, \omega_2)\mathrm{d}\omega_2\mathrm{d}\omega_1\mathrm{d}\theta}{V_2^2} +$$
$$\int_0^{\frac{\pi}{2}} \int_{-\frac{\pi}{2}}^{\theta - \frac{\pi}{2}} \int_{-\omega_1}^{\frac{\pi}{2}} \frac{2f\left(\omega_1, \omega_2\right)\mathrm{d}\omega_2\mathrm{d}\omega_1\mathrm{d}\theta}{V_3^2} + \int_{-\frac{\pi}{2}}^{0} \int_{-\frac{\pi}{2}}^{\theta} \int_{-\omega_1}^{\frac{\pi}{2}} \frac{2f\left(\omega_1, \omega_2\right)\mathrm{d}\omega_2\mathrm{d}\omega_1\mathrm{d}\theta}{V_4^2},$$

where

$$V_1 = \frac{2\theta + \sin(2(\theta - \omega_1)) + \sin(2\omega_1)}{2\cos^2\omega_1} + \frac{\pi + 2\omega_2 + \sin(2\omega_2)}{2\cos^2\omega_2}$$
$$V_2 = \frac{2\theta + \sin(2(\theta - \omega_1)) + \sin(2\omega_1)}{2\cos^2\omega_1} + \frac{2\pi - 2\theta + \sin(2\omega_2) - \sin(2(\theta + \omega_2))}{2\cos^2\omega_2}$$
$$V_3 = \frac{\pi + 2\omega_1 + \sin(2\omega_1)}{2\cos^2\omega_1} + \frac{2\pi - 2\theta + \sin(2\omega_2) - \sin(2(\theta + \omega_2))}{2\cos^2\omega_2}$$
$$V_4 = \frac{\pi + 2\theta + 2\omega_2 + \sin(2(\theta + \omega_2))}{2\cos^2\omega_2}.$$

Proof. We consider same coordinate system with Lemma 5, with the seed S_0 being the origin. We separate between angles $-\frac{\pi}{2} \leq \theta \leq \frac{\pi}{2}$ and $\frac{\pi}{2} \leq \theta \leq \frac{3\pi}{2}$. Due to symmetry, it is sufficient to carry out the computation only for $-\frac{\pi}{2} \leq \theta \leq \frac{\pi}{2}$. For $0 \leq \theta \leq \frac{\pi}{2}$, all configurations of points P_1, P_2 can be divided into three cases: Both points are located at the upper-right quadrant, $\left\{\phi_1 \leq \frac{\pi}{2}, \phi_2 \leq \frac{\pi}{2}\right\}$, point P_1 is located at the upper-right and point P_2 at the upper-left quadrant, $\left\{\phi_1 \leq \frac{\pi}{2}, \frac{\pi}{2} \leq \phi_2 \leq \pi\right\}$, and both points are located at the upper-left quadrant, $\left\{\frac{\pi}{2} \leq \phi_1 \leq \pi, \frac{\pi}{2} \leq \phi_2 \leq \pi\right\}$. An example configuration for the first case is depicted in Fig. 6(a),
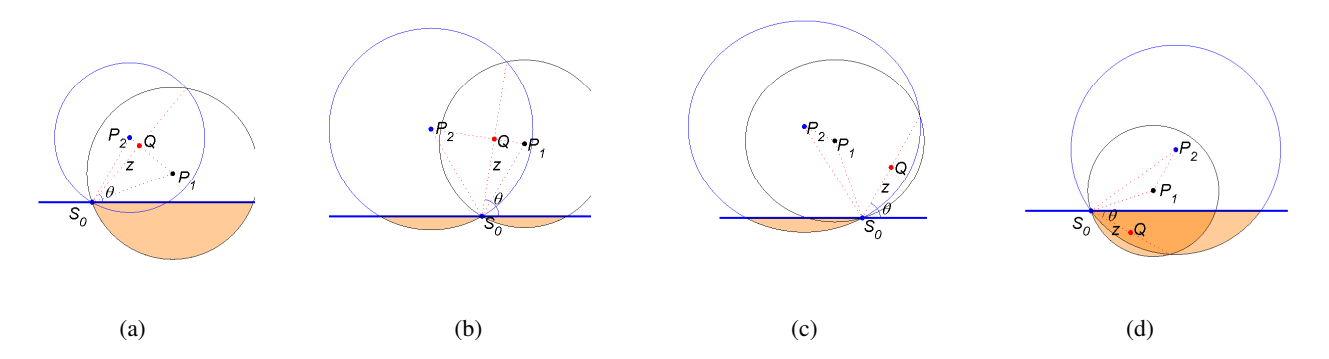
Fig. 6. Coordinate systems and example illustrations of the void area around two interior points P_1, P_2 when the seed S_0 is located at the boundary of the half-plane.

where the void due to the point P_2 is not anymore limited from a boundary along the y-axis, thus

$$V_1 = \frac{2\theta + \sin\left(2\left(\theta - \omega_1\right)\right) + \sin\left(2\omega_1\right)}{2\cos^2\omega_1} + \frac{\pi + 2\omega_2 + \sin\left(2\omega_2\right)}{2\cos^2\omega_2}.$$

In the second case, both voids due to points P_1 and P_2 are truncated from the boundary, see Fig. 6(b). After some straightfoward calculation we get the size of the associated void,

$$V_2 = \frac{2\theta + \sin\left(2\left(\theta - \omega_1\right)\right) + \sin\left(2\omega_1\right)}{2\cos^2\omega_1} + \frac{2\pi - 2\theta + \sin\left(2\omega_2\right) - \sin\left(2\left(\theta + \omega_2\right)\right)}{2\cos^2\omega_2}.$$

In the third case, see Fig. 6(c), only the void of point P_2 is affected from the boundary

$$V_3 = \frac{\pi + 2\omega_1 + \sin\left(2\omega_1\right)}{2\cos^2\omega_1} + \frac{2\pi - 2\theta + \sin\left(2\omega_2\right) - \sin\left(2\left(\theta + \omega_2\right)\right)}{2\cos^2\omega_2}.$$

Finally, for $\theta < 0$, see Fig. 6(d), the void is determined only from point P_2 and $V_4 = \frac{\pi + 2\theta + 2\omega_2 + \sin(2(\theta + \omega_2))}{2\cos^2\omega_2}$. After multiplying every term by four to consider angles $\frac{\pi}{2} \leq \theta \leq \frac{3\pi}{2}$ and to count every pair of points twice and summing up we get the result of the Lemma. $\square$

After carrying out the numerical integration we get $\mathbb{E}\left\{A^2\right\} = 0.23781$ in Lemma 5 and $\mathbb{E}\left\{A^2\right\} = 0.54508$ in Lemma 6. The associated mean values at the corner of the quadrant and at the boundary of the half-plane are given in equations (5) and (7) respectively. After fitting the first two moments of the cell size to the Gamma distribution, $\frac{x^{k-1}e^{-x/\nu}}{\nu^k\Gamma(k)}$, one can compute the parameters $k = \frac{\mathbb{E}\{A\}^2}{\mathbb{V}\mathrm{ar}\{A\}}$ and $\nu = \frac{\mathbb{E}\{A\}}{k}$, and use them to approximate the distribution of the cell size.

The mean and the variance of the cell size as well as the Gamma parameters k, ν at the corner of the quadrant, at the edge of the half-plane, and in the infinite plane (i.e. in the bulk)

TABLE I

FITTING THE GAMMA DISTRIBUTION TO THE DISTRIBUTION OF THE SIZE OF THE CELL $\mathcal{C}_0$.

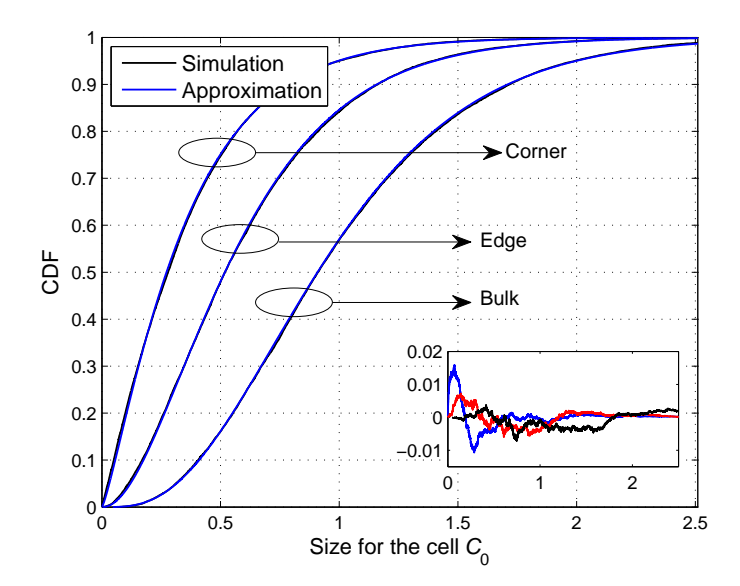|	$\mathbb{E}\{A\}$	$\mathbb{V}\text{ar}\{A\}$	k	ν
Corner	0.36351	0.10567	1.25052	0.29069
Edge	0.61082	0.17198	2.16935	0.28157
Bulk	1	0.28018	3.56918	0.28018

Fig. 7. Distribution of the area of the Voronoi cell $\mathcal{C}_0$ at different locations using simulations and the Gamma distribution with fitted parameters, see Table I. In the subfigure, we depict the approximation error between the simulated and approximated CDF, i.e., $F_{\text{sim}} - F_{\text{app}}$, where F is the CDF, at the corner (blue), at the edge (red) and in the bulk (black). It indicates that with the selected parameters the distributions are not Gamma.

are summarized in Table I. We see that the parameter k depends clearly on the location while the parameter ν is not that sensitive. In the bulk, it is already known that the Gamma distribution gives a good fit with parameters $k = \nu^{-1} = 3.61$ [8] estimated by simulations, and $k = \nu^{-1} = 3.575$ [22] estimated by integration. These values are also close to the parameters in Table I. The parameterized Gamma distributions at the corner and at the edge are to the best of our knowledge new. In Fig. 7, we have simulated $10\,000$ PVTs over a square with side $L = 10$ and PPP intensity equal to unity. We see that the Gamma distribution with fitted mean and variance provides a good approximation for the distribution of the cell size also at the corner and at
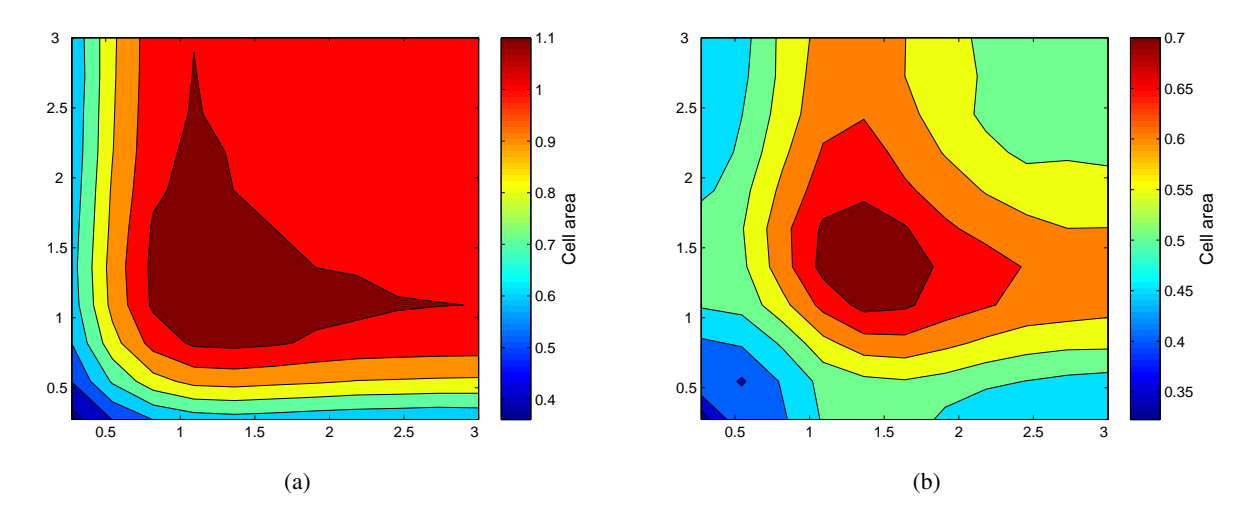
Fig. 8. Contour plots for (a) the mean, and (b) the standard deviation of the cell size close to the corner of the quadrant. A grid of 11×11 seeds is simulated with $100\,000$ simulations per seed. The corner of the quadrant has coordinates $(0, 0)$.

the edge. The simulated mean and variance at the corner are 0.36125 and 0.10271 respectively, while at the edge the related values are 0.60796 and 0.16928.

The numerical calculation of the mean and the variance of the cell size close to the boundary and the corner of the quadrant involves the size of void areas which are tedious to express in closed-form. In Fig. 8, we have simulated the contour plots for the mean and the standard deviation of cell size for a grid of seeds close to the corner of the quadrant. The coordinates of the seed S_0 are $(i\Delta x, j\Delta y)$, where $\Delta x = \Delta y = 0.3$ and $i = 0, 1, \ldots, 10, j = 0, 1, \ldots, 10$. As expected, the mean and the variance of the cell size are maximized when the seed is located close to the boundary and also close to the corner of the quadrant. In addition, we see in Fig. 8(a) that the mean cell size converges quickly to unity as we move towards the bulk.

V. APPLICATION TO SECRECY

Physical layer security without exchanging secret keys was first proposed by Wyner [19] and refers to the protection of information messages against eavesdropping with the aid of channel coding. Physical layer security would be well-suited for devices with light computational power, e.g., in certain types of sensor networks, where conventional security techniques, e.g., based on cryptography fail to adapt due to their high complexity [23].

Let us consider an entity A that wants to send a message to entity B. The message is protected against the i-th eavesdropper E_i, if the eavesdropper fails to extract useful information from the

message it receives. We will assume that A succeeds to send the message in a secure manner, if the distance between A and B is smaller than the distance between A and the eavesdropper closest to A, i.e., $d(A, B) < d(A, E_i) \forall i$. The distance-based criterion for secure connectivity corresponds to the case where the fading statistics are neglected, the noise power levels at the legitimate users and at the eavesdroppers are equal, and the secrecy rate threshold is zero [17].

We consider the PPPs of legitimate users, Π_l, and eavesdroppers, Π_e, with densities λ_l and λ_e. Let $p = \frac{\lambda_l}{\lambda_e}$. We place a *virtual node* at S_0, either at the corner of a quadrant or at the edge of the half-plane, to study secure in- and out-connectivity at that location. For instance, this could be the location of an aggregator where all sensors (legitimate users) want to transmit measurement data. The number of legitimate users connected securely to the *virtual node* describes the in-degree with secrecy. We will study the moments of the in-degree and its Probability Mass Function (PMF) over the ensemble of all possible realizations of Π_l, Π_e.

A legitimate user has secure in-connection to the *virtual node*, if their distance separation is smaller than the distance between that user and any eavesdropper [17]. The in-degree accepts an elegant geometric interpretation using the PVT: It is equal to the number of legitimate users that fall inside the Voronoi cell $\mathcal{C}_0$ of the point process $\Pi_e \cup \{S_0\}$ [17]. Conditioned on the size of the cell $\mathcal{C}_0$, the Random Variable (RV) describing the in-degree, N_{in}, follows the Poisson distribution $\text{Po}(\lambda_l |\mathcal{C}_0|)$ or $\text{Po}(pA)$, where A is the size of cell $\mathcal{C}_0$ induced by a unit intensity PPP.

The mean and the variance of the in-degree can be expressed in terms of the moments of the cell size $\mathbb{E}\{A\}$ and $\mathbb{E}\{A^2\}$. One has to average the mean and variance of the Poisson distribution $\text{Po}(pA)$ over the cell size A

$$\begin{aligned} \mathbb{E}\{N_{\text{in}}\} &= p\,\mathbb{E}\{A\} \\ \mathbb{V}\text{ar}\{N_{\text{in}}\} &= p\,\mathbb{E}\{A\} + p^2\,\mathbb{E}\{A^2\} - p^2\mathbb{E}\{A\}^2. \end{aligned} \tag{10}$$

Lemma 7. *The probability of in-isolation can be approximated as* $\mathbb{P}_{in\text{-}isol} \approx \frac{1}{(1+p\nu)^k}$, *where* k, ν *are parameters of the Gamma distribution shown in Table I.*

Proof. The PMF of the in-degree $f_{N_{\text{in}}}(n)$ can be approximated after averaging the Poisson distribution $\text{Po}(pA)$ over the Gamma approximation for the PDF of the cell size A.

$$f_{N_{\text{in}}}(n) \approx \int_0^\infty \frac{(p\,A)^n\, e^{-p\,A}}{n!} \frac{A^{k-1} e^{-A/\nu}}{\nu^k \Gamma(k)} \mathrm{d}A = \frac{(p\,\nu)^n\, \Gamma(k+n)}{n!\, \Gamma(k)\, (1+p\,\nu)^{n+k}}.$$

Using the Gamma approximation, the probability of in-isolation is obtained after setting $n = 0$ users with secure in-connectivity in the PMF calculated above; $\mathbb{P}_{\text{in-isol}} \approx f_{N_{\text{in}}}(0) = \frac{1}{(1+p\,\nu)^k}$. $\qquad\square$
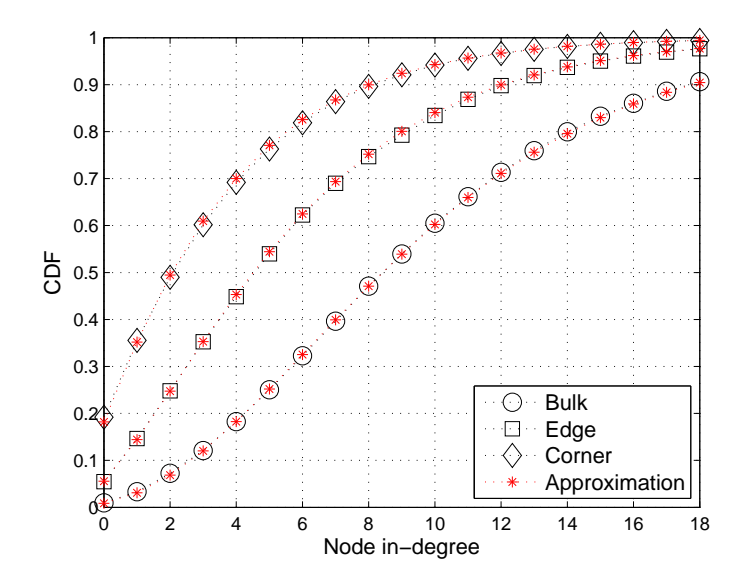
Fig. 9. CDF of the in-degree with physical layer security at different locations. The intensities for the legitimate users and the eavesdroppers are $\lambda_l = 10$ and $\lambda_e = 1$. In the simulations, we consider a square with side $L = 10$ and we place the virtual node at the corner $(0,0)$, at the edge $(L/2, 0)$, and in the middle of the square $(L/2, L/2)$. In the approximations, equation (11) is used with parameters k, ν available in Table I for the different locations.

The CDF of the in-degree can be expressed in terms of the Gaussian hypergeometric function $_2F_1$, see for instance [24, pp. 556]

$$F_{N_{\text{in}}}(n) \approx 1 - \frac{(p\,\nu)^{1+n}\,\Gamma\left(1+k+n\right)\,_2F_1\left(1, 1+k+n; 2+n; \frac{p\,\nu}{1+p\,\nu}\right)}{(1+p\,\nu)^{1+k+n}\,\Gamma\left(k\right)\Gamma\left(2+n\right)}. \tag{11}$$

In Fig. 7 we depict the approximation accuracy of equation (11) at the corner, at the edge and in the bulk, with parameters k, ν available in Table I.

The number of legitimate users where the *virtual node* can securely transmit to describes the out-degree with secrecy. Following the same assumptions used to study in-connectivity with secrecy, the *virtual node* can securely transmit to a legitimate user if their distance is smaller than the distance between the *node* and any eavesdropper. The distribution of the out-degree is independent of the location S_0 of the *node*: The quantity $\frac{\lambda_l}{\lambda_e + \lambda_l} = \frac{p}{1+p}$ is the probability that the next user we meet as we move away from the *node* is legitimate. Therefore the out-degree is equal to n if we succeed in meeting n legitimate users before the first eavesdropper. It follows that the distribution of the out-degree is Geometric with parameter $\frac{p}{1+p}$ [17], [25].

$$f_{N_{\text{out}}}(n) = \left(\frac{p}{1+p}\right)^n \frac{1}{1+p}, \quad F_{N_{\text{out}}}(n) = 1 - \left(\frac{p}{1+p}\right)^{1+n}, \quad n \geq 0. \tag{12}$$

From equations (12) we get $\mathbb{E}\{N_{\text{out}}\} = p, \mathbb{V}\text{ar}\{N_{\text{out}}\} = p(1+p)$, and the probability of out-isolation is $\mathbb{P}_{\text{out-isol}} = f_{N_{\text{out}}}(0) = \frac{1}{1+p}$.

Lemma 8. *In areas with boundaries the mean in- and out-degree with secrecy are not necessarily equal.*

Proof. Since $\mathbb{E}\{A\} < 1$ along the boundary of a quadrant, see Lemma 2, $\mathbb{E}\{N_{\text{out}}\} = p > p\,\mathbb{E}\{A\} \stackrel{(a)}{=} \mathbb{E}\{N_{\text{in}}\}$, where (a) follows from equation (10). On the other hand, close to the boundary and far from the corner, we may have $\mathbb{E}\{A\} > 1$, see Lemma 4, thus $\mathbb{E}\{N_{\text{out}}\} < \mathbb{E}\{N_{\text{in}}\}$. Finally, in the bulk, $\mathbb{E}\{A\} = 1$, and $\mathbb{E}\{N_{\text{out}}\} = \mathbb{E}\{N_{\text{in}}\} = p$. $\qquad\square$

The relation between the probabilities for in- and out-isolation depends on the location and the intensity ratio p. Verifying the results in [17], it is more probable to be in-connected than out-connected in the bulk, see Fig. 10. However, this is not true in general. In Fig. 10 we see that at the corner of a quadrant and at the edge of the half-plane it is more likely to be out-connected than in-connected (for a moderate to high intensity of eavesdroppers). A single eavesdropper located close to the *virtual node* makes it out-isolated, while the *virtual node* can still be in-connected provided that legitimate users are located far from the eavesdropper. At the corner and at the edge, the probability to be in-connected is reduced, because the possible locations for the legitimate users close to the boundaries are less as compared to the bulk.

VI. CONCLUSIONS

Instead of using extensive simulations, this letter uses a low-complexity numerical method for computing the mean cell size in a homogeneous Poisson Voronoi tessellation for seeds located along and/or close to the boundary of a quadrant. Besides the application on physical layer security detailed in the paper, these results can also be used in the performance analysis of finite area cellular networks, e.g., modeling the mean network load for base stations located close to the network borders. In the foreseen deployments of indoor ultra-dense networks, the impact of boundaries cannot be neglected. In addition, the calculation of the second moment of the cell size at the corner of a quadrant and at the boundary of the half-plane, and the illustration of the good fit of the Gamma distribution, may give enough evidence to continue studying the distribution of cell size in other locations and more complex bounded geometries, e.g., three-dimensional Voronoi cells, cell size distribution in hyperbolic spaces, etc.
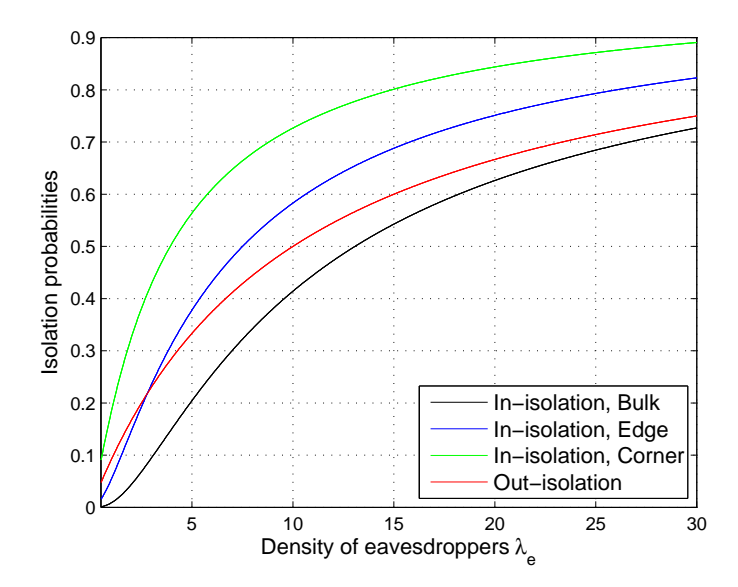
Fig. 10. Probability of isolation w.r.t. to the intensity of eavesdroppers while the intensity of legitimate users is $\lambda_l = 10$. The probability of in-isolation is approximated by $\mathbb{P}_{\text{in-isol}} \approx \frac{1}{(1+p\,\nu)^k}$. The probability of out-isolation is $\mathbb{P}_{\text{out-isol}} = \frac{1}{1+p}$.

REFERENCES

[1] J. Møller, "Random tessellations in Rd", *Advances in Applied Probability*, vol. 21, pp. 37-73, 1989.

[2] V.M. Lieshout, "An introduction to planar random tessellation models", *Spatial Statistics* vol. 1, pp. 40-49, 2012.

[3] F.P. Schoenberg, C. Barr, and J. Seo, "The distribution of Voronoi cells generated by southern California earthquake epicenters", *Environmetrics*, vol. 20(2) p. 159-171, 2008.

[4] M. Ramella *et. al.*, "Finding galaxy clusters using Voronoi tessellations", DOI: 10.1051/0004-6361:20010071, 2001.

[5] F. Baccelli, and B. Błaszczyszyn, "On a coverage process ranging from the Boolean model to the Poisson Voronoi tessellation with applications to wireless communications", *Advances Applied Probabability*, vol. 33, pp. 293-323, 2001.

[6] J.L. Meijering, "Interface area, edge length, and number of vertices in crystal aggregates with random nucleation", Philips Res. Rep. 8, 270-290, 1953.

[7] E.N. Gilbert, "Random subdivisions of space into crystals", Annals of Mathematical Statistics 33, 958-972, 1962.

[8] D. Weaire, J.P. Kermode and J. Wejchert, "On the distribution of cell areas in a Voronoi network", *Philosophical Magazine Part B*, 53:5, L101-L105, DOI: 10.1080/13642818608240647.

[9] M. Tanemura, "Statistical distributions of Poisson Voronoi cells in two and three dimensions", *Forma*, vol. 18, no. 4, pp. 221-247, 2003.

[10] S. Kumar, S.K. Kurtz, J.R. Banavar, and M.G. Sharma,"Properties of a three-dimensional Poisson Voronoi tessellation: A Monte-Carlo study ", *Journal of Statistical Physics*, vol. 67, Nos. 3/4, 1992.

[11] J.S. Ferenc and Z. Neda, "On the size distribution of Poisson Voronoi cells," *Physica A: Statistical Mechanics and its Applications*, vol. 385, no. 2, pp. 518-526, 2007.

[12] K.A. Brakke, "Statistics of random plane Voronoi tessellations", *unpublished*, available at http://facstaff.susqu.edu/brakke/aux/downloads/papers/vorplane.pdf.

[13] P.N. Rathie, "On the volume distribution of the typical Poisson-Delaunay cell", *Journal of Applied Probability*, vol. 29(3), pp. 740-744, 1992.

[14] L. Muche, "Distributional properties of the three-dimensional Poisson Delaunay cell", *Journal Statistical Physics*, vol. 84, 1996.

[15] J.G. Andrews, F. Baccelli, and R.K. Ganti, "A Tractable approach to coverage and rate in cellular networks", *IEEE Transactions on Communications*, vol. 59, Nov. 2011, pp. 3122-3134.

[16] D. Cao, S. Zhou, and Z. Niu, "Optimal combination of base station densities for energy-efficient two-tier heterogeneous cellular networks", *IEEE Transactions Wireless Communications*, vol. 12, Sept. 2013, pp. 4350-4362.

[17] P.C. Pinto, J. Barros, and M.Z. Win, "Secure communication in stochastic wireless networks − Part I: Connectivity", *IEEE Transactions Information Forensics and Security*, vol. 7, no. 1, pp. 125-138, Feb. 2012.

[18] L. Devroye, L. Györfi, G. Lugosi, and H. Walk, "On the meansure of Voronoi cells", *Journal of Applied Probability*, vol. 54(2), pp. 394-408, 2017.

[19] A.D. Wyner, "The wire-tap channel", *The Bell System Technical Journal*, vol. 54, no. 8, pp. 1355-1387, Oct. 1975.

[20] D. Stoyan, W. S. Kendall, and J. Mecke, "Stochastic geometry and its applications", ISBN 0-471-95099-8, 1995.

[21] A. Hayen, and M.P. Quine, "Areas of components of a Voronoi polygon in a homogenenous Poisson process in the plane", *Advances in Applied Probability*, vol. 34, no. 2, pp. 281-291, 2002.

[22] E. Pineda, P. Bruna, and D. Crespo, "Cell size distribution in random tessellations of space", *Physical Review E*, 70, 066119, 2004.

[23] W. Trappe, "The challenges facing physical layer security", *IEEE Commun. Magazine*, vol. 53, pp. 16-20, Jun. 2015.

[24] M. Abramowitz, and I.A. Stegun. Handbook of mathematical functionswith formulas, graphs and mathematical tables. 1972.

[25] M. Haenggi, "The secrecy graph and some of its properties", *IEEE International Symposium Information Theory*, pp. 539-543, 2008.